3D Mapping and Stability Prediction for Autonomous Wheelchairs

Aryan Naveen, Haitao Luo, Zhimin Chen, Bing Li*

Department of Automotive Engineering, Clemson University
International Center for Automotive Research (CU-ICAR)
4 Research Dr., Greenville, SC 29607, USA. Email: bli4@clemson.edu

***Abstract*—Autonomous wheelchairs can address a very large need in many populations by serving as the gateway to a much higher degree of independence and mobility capability. This is due to the fact that the big picture idea for autonomous wheelchairs integration into the transportation chain is to allow for individuals to be able to utilize the Intelligent wheelchair to reach the vehicle (regardless of terrain), mount into autonomous wheelchair that navigates to desired destination, and finally autonomous wheelchair dismounts. This will enable a higher degree of mobility for a handicapped population that experiences a large quantity of restrictions as a result of their circumstances. In order for this potential to be achieved numerous precautions must be integrated into the control system, such as stability maintenance. This paper focuses on mapping the environment through the use of a LiDAR sensor and predicting the stability of the given wheelchair. We utilize RTAB Mapping in combination with LiDAR odometry to construct a 3D map of the environment. Then Poisson reconstruction is deployed to convert the built 3D pointcloud into triangular mesh that allows for the norms to the surface to be calculated, which allows for stability prediction. This paper, not only outlines a novel pipeline but also deployed the pipeline on the recently released Intel RealSense L515 sensor and leverages its unique capabilities.**

***Keywords*—LiDAR-Camera, SLAM, 3D Mapping, Mesh Mapping, Dynamic Model, Wheelchair Stability**

I. Introduction

Autonomous wheelchairs can serve as a bridge to a completely different level of mobility for the physically handicapped population [1]. By enabling wheelchair traversal capabilities, eventually individuals with disabilities preventing them from being able to walk/drive will be able to function at a much higher level independently. Mapping and understanding the environment are crucial roles to ensuring the stability of the wheelchair as a method of preventing harm for the user.

Obstacle avoidance [2] is only one part of the challenge of autonomous wheelchair control, because in addition to obstacles mapping terrains that can pose hazards to the wheelchair due to unstable orientations is also crucial. In order for this to be achieved effective 3D mapping [3] of the environment must be performed to gather the data in a form from which analysis can be performed. There are two main challenges in this big picture challenge: accurately mapping the environment with large data noise levels present and representing the wheelchair and environment interaction. The conditions that merit an unstable configuration must be defined in terms of a specific wheelchair's parameters rather than a generalized definition as each wheelchair is unique.

On the data collection side there are a wide variety of technologies and algorithms available to gather data on the surroundings. For instance, there are visual based means of determining depth through the use of stereo camera. Although there are a multitude of options in the above category such as the RealSense D435i [4] and Kinect cameras [5], in this paper LiDAR technology was leveraged through a recently released sensor by Intel RealSense L515 [6]. This sensor, offers a much more affordable means to LiDAR technology that is capable of performing accurate mapping for the purposes required by an autonomous wheelchair. Furthermore, unlike visual based depth data, the LiDAR sensor will work regardless of lighting conditions which will further enable greater independence for the user. In addition, within the L515 there in an inertial measurement unit (IMU) which is fused with the LiDAR odometry for accurate pose estimation of the autonomous wheelchair.

Leveraging our previous research in [7], we extend our approach to a more generic 3D reconstruction pipeline to utilize lidar based depth data to construct a 3D map and eventually triangular mesh of the surrounding terrain. Specifically, RTAB mapping [8] is employed with LiDAR odometry to construct a 3D pointcloud of the environment and then converted to mesh through Poisson reconstruction. The mesh easily offers the gradient of the terrain which is used to predict the stability of the wheelchair.

II. Related work

A. Wheelchair 3D Mapping

In order for effective navigation in an outdoor environment a multitude of information is required. The data serves a multitude of roles that ranges from localization [4] to obstacle detection [2]. The most direct motivation behind a multi-layer map is for localization and navigation purposes. Multiple research works have focused on building different 3D maps of a given environment with different information for the wheelchair. Murakara et. al analyzed the integration of vision and laser range finders to construct a 2 dimensional indoor safety map for a wheelchair [9]. Their work focused on extracting various features like fixed obstacles (walls, tables, et. al), dynamic obstacles (people), rough surfaces, et, al from a given environment to be able to produce a map in reference to the safety of the autonomous wheelchair. Recent progress on the SLAM(Simultaneous localization and mapping) [10] and three dimensional map generation has also been very promising. Zhao et. al implemented a graph based SLAM

approach for building a grid point cloud semantic map for indoor navigation of an autonomous wheelchair [11]. In our work we need to perform 3D mapping with the end goal of stability analysis for a wheelchair as compared to other's work which focused more on the navigation aspect of autonomous wheelchairs.

In addition, within constructing the 3D map of the environment a crucial concept that is well studied is odometry and pose estimation using the location of environmental landmarks. The most significant and accessible technique is Visual odometry [12], which essentially estimates the pose of the sensor in real time through the use of sequential RGB images. From these images, extract environmental features and create a transformation between images based on the change in these features position in the image. Although, this technique has a wide expanse of merits, this paper utilizes LiDAR odometry through Iterative Closest Point (ICP) [13]. In a similar fashion to visual odometry, this technique determines the transformation from frame to frame, however it uses the change in 3D pose of the environmental feature as it's basis rather than the change in the 2D image.

Furthermore, for mesh generation [14] there are numerous developed algorithms for producing triangular mesh from a given pointcloud. In a situation where run time is important, methods like Delaunay Triangulation [15] and Alpha Shapes [16] are used. The logic behind Delaunay Triangulation is essentially to project all points in a pointcloud onto a 2-dimensional plane to produce P there exists a triangulation $DT(P)$ such that no point in P is inside the circumcircle of any triangle in DT(P). Delaunay triangulations maximize the minimum angle of all the angles of the triangles in the triangulation; they tend to avoid sliver triangles. Although this algorithm runs in log time, frequently it requires additional smoothing and are very poor performers when presented with noisy data as they attempt to overcompensate for those points.

B. Wheelchair Rollover Stability

Dynamic and static vehicle rollover models are crucial for rollover prediction and control. In a static rollover stability analysis, numerous factors can be considered including lateral acceleration, roll angle, and roll rate. Furthermore, T-static stability factor is a ratio between the track of the vehicle and the centroid height, which is used to indicate the maximum lateral acceleration [17]. In addition, another important phenomenon in stability analysis is that of load transfer, which describes the shift in distribution of the vehicle's weight between the wheels [18]. Dynamic modeling has been performed for a variety of different vehicles including all-terrain vehicles (ATVs) and three wheeled vehicles [17]. In addition, modeling has been performed to account for various types of suspensions, chassises, and drive systems [19] [18]. In our case we treat the wheelchair as a rigid body and do not need to account for these factors as wheelchairs use simple differential drive without any suspension thereby simplifying the model. Furthermore, specific to wheelchairs, Candiotti et. al perform stability analysis with their novel electric power wheelchair, MEBot, based on analyzing the movement of the center of mass of the wheelchair [20].

Moreover, in the analysis of vehicular stability there are two categories for rollover: tripped and untripped [18]. In the case of untripped, the cause of rollover is the actual motion of the wheelchair, such as turning too fast. In the case of a tripped rollover an object in the terrain caused an orientation of the wheelchair where it could no longer maintain stability and thus tipped over.

In addition, since performing rollover analysis is crucial for developing safe and effective automated control systems much effort has been put into investigating rollover propensity and the cause for vehicle rollover. However, since rollover experimental tests are dangerous and expensive to perform, many researchers have studied methods for testing vehicle dynamics and control systems for preventing rollover. This challenge has been addressed by two methods: small scale tests and simulations. [21] and [22] utilize small scale replicas for stability analysis, however a potential flaw with such a method is there is no guarantee the dynamic properties observed in scaled replica mirror those of actual size. The other method utilized is simulation which is also used by [23] (TruckSim). For our experimental purposes MSC ADAMS software was utilized to perform simulations to assess stability of the wheelchair.

III. Environment 3D mapping

A. 3D Mapping using SLAM

For the purposes of contructing a three dimensional representation of the surrouding terrain of the autonomous wheelchair RTAB mapping [8] was employed, which utilizes graph based SLAM. The essence of RTAB mapping is that at each node, the corresponding depth pose of the sensor , x_i, and the raw data, D, at a specific time step t, while a link contains the measurement constraints w_t and v_t. With regards to calculating the pose, either visual odometry or LiDAR based odometry is used in addition to the IMU to predict the pose of the sensor. In the optimization phase, a maximum likelihood estimation (MLE) algorithm is deployed to determine the most likely configuration of locations based on the observed data to minimize the contraints in the links. The constraints at time step t, for pose x_t and sensor reading, z_t, are given by

$$v_t = z_t - h(x_t, m_t) \tag{1}$$

$$w_t = x_t - g(x_{t-1}, u_t) \tag{2}$$

where h() and g() represent the measurement and motion functions and Q_t and R_t are the covariances of the measurement and motion noise. Then the optimal graph configuration can be solved by minimizing the following relation.

$$J_{graphSLAM} = x_0^T{}_0 + \sum_t w_t^T R_T^{-1} w_t + v_t^T Q_T^{-1} v_t \tag{3}$$

The goal of graph SLAM is to create a graph of all robot poses and features encountered in the environment and compute the most likely robot's path and map of the environment. Furthermore, the RTAB algorithm can be split into three aspects: front-end, back-end, and loop closure detection.

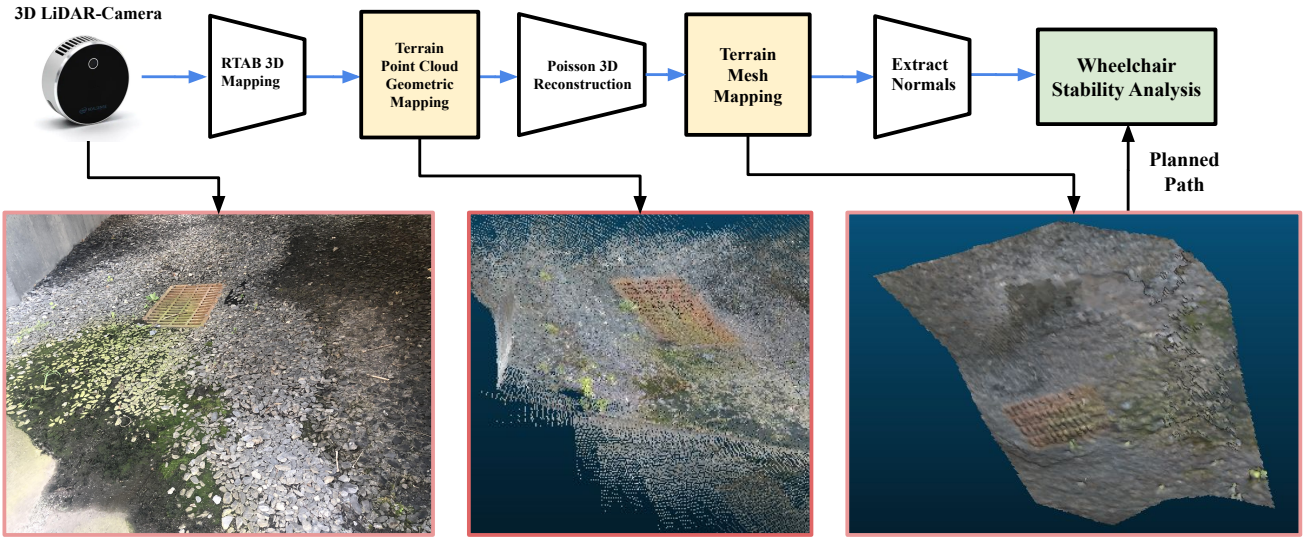

Fig. 1: Terrain LiDAR-camera based 3D Mapping and stability analysis for wheelchair

1) Front-end of RTAB Algorithm: The front-end of RTAB is focused on constructing the graph using data collected. For our pipeline, we choose to use an Intel RealSense LiDAR Camera L515 to perform 3D Mapping of the safety zone. The Intel RealSense L515 provides dense depth data based on the LiDAR sensor along with an additional IMU odometry fused with either visual or LiDAR based odometry (see subsection III-A4). At time steps t, we store the depth calculated from the stereo image, along with the pose gathered from the internal IMU in a new node (Figure 1). Furthermore, the front-end in the RTAB algorithm attempts to solve the data association problem by detecting loop closures.

2) Back-end of RTAB Algorithm: The back-end of the RTAB algorithm is where all the main optimization happens. The algorithm takes the complete graph of nodes and links and computes the most likely configuration following the above constraint $J_{graphSLAM}$.

3) Loop-closure Detection: The loop-closure detection algorithm employed using bag-of-words approach described in [8]. Essentially, every time a node is created visual features are extracted and quantized to incremental visual vocabulary. Then, since RTAB generates a global graph of nodes and links, the visual features in node generated a time step t is compared to nodes generated prior to determine a match. To compute the likelihood of a match , Tf-IDF approach proposed by Sivic [24], is used to update a Bayes filter estimating the loop closure hypotheses. The filter estimates if the new node is from a previously visited location or a new location. When a loop closure hypothesis reaches the fixed threshold, a loop closure is detected and transformation is computed.

4) Odometry: With regards to the odometry component of 3D mapping, use of a LiDAR based sensor offers two main options for environment based odometry: LiDAR and visual. With regards to visual odometry, through the use of RGB images landmarks in the environment can be tracked to provide an estimate of the sensor's pose in the environment. In a similar fashion, ICP or LiDAR based odometry uses pointcloud data and tracks 3D landmarks updated pose to be able to predict the sensor's pose as well. A couple major limitations of visual based odometry is the fact that it cannot be performed in a dark environment as it is dependent upon RGB image information and without light there is no data therefore in this paper, LiDAR based odometry was used in union with the internal IMU of the L515.

B. 3D Mesh Generation

The purposes of mesh generation is to create a representation for the gathered pointcloud that conforms to the defining geometric charactistics of the environmental terrain. In this paper Poisson Surface Reconstruction [25], proposed by Kazhdan et. al, as it is highly resilient to data noise which will be encountered in a generated 3D map from an outdoor environment. Essentially, Poisson reconstruction attempts to solve for an indicator function to represent the pointcloud based on the vector field, as outlined in [7].

Furthermore Poisson Triangulation runs in polynomial time therefore prior to performing mesh generation we subsample the built 3D map, K percent of the points.

IV. Dynamic Model of the Wheelchair Rollover Stability

The modeling process is based on the following assumptions:

1) The wheelchair as a whole is treated as a rigid body in the calculations
2) The distribution of mass in the wheelchair is symmetrical across the middle plane of the wheels on both sides, where the center of mass lies.
3) The four-wheeled wheelchair model can be simplified to a two-wheeled model, where the two wheel contact points are the same as a longitudinal middle spot, and the center of mass lies of this plane.

These are the same assumptions that are made in [7], therefore the same dynamic model representation of the wheelchair is utilized in this paper.

A. Maximum roll angle a_{max}^{static}

When the gradient of the slope reaches the static maximum roll angle of the wheelchair, a_{max}^{static}, all the weight of the wheelchair is supported by the tire at contact point A which leads to the following relationship as shown in [7].

$$a_{max}^{static} = \tan^{-1} \frac{B}{2h_s} \tag{4}$$

B. Wheelchair dynamic rollover threshold $\frac{a_y}{g}$

When the wheelchair is about to roll over, the normal force on the wheels on the outside is zero. Once again following the same procedure in [7], we arrive at the following expression:

$$\frac{a_y}{g} = \frac{B}{2h_s} \tag{5}$$

The above formula (5) is the roll threshold value when the wheelchair is in a steady state condition which is used to evaluate the wheelchair's anti rollover capability.

C. Dynamic Model with Generated Mesh

Using the generated mesh, along with the dynamic model of the wheelchair, paths for the wheelchair can be planned to ensure stability of the user. Using the generated mesh calculate the normals for every vertices by taking the cross product of the edges that touch connect to that vertex N. Represent N, in terms of spherical coordinates (r, θ, ϕ), and if θ ever exceeds the critical angle calculated in the dynamic model for the wheelchair then the wheelchair is not stable at that point.

V. Experiment

In this section we outline the experiment in which the proposed algorithm (Figure 1) was used to generate a 3D triangular mesh to represent a variety of different terrains/obstacles that could be seen by an autonomous wheelchair in an urban environment. These terrains fell into two categories: traversable and non-traversable. Simulations in ADAMs were performed to verify our hypothesis surrounding whether the wheelchair could handle certain geometric characteristics of a terrain.

A. Field Data Collection

For the data collection using the L515, we implemented the SLAM based 3D mapping approach outlined above to construct maps of various terrains deployed on the wheelchair shown in Figure 2. The wheelchair, is equipped with an outward facing Intel RealSense L515 for data collection of the environment in addition to an Intel RealSense D435i camera facing the user for hmi purposes. In this paper, the LiDAR sensor was used to map a wide variety of terrains to evaluate the various components of the proposed pipeline including: mesh quality, stability prediction, and odometry. The wheelchair runs Ubuntu 16.04 with ROS kinetic, therefore the pipeline was deployed on that system.

Fig. 2: Automated wheelchair used in experiments video [1]

B. 3D Mapping and Mesh Result

In order to evaluate the quality of the various mesh generation techniques, Edge Root Mean Square (ERMS) in formula (6) was used as the quality metric. The results shown in Table I indicate that Poisson reconstruction produced mesh representations that were an effective representation for the 3D map while keeping the geometric characteristics of the data (Figure 1). The

$$ERMS_{\mu} = \frac{1}{N} \sum_{t \in \Lambda_t} \sqrt{\frac{t_{L1}^2 + t_{L2}^2 + t_{L3}^2}{3}} \tag{6}$$

where Λ_T is the set of all triangles that make up the different meshes, and t_{L1}, t_{L2}, t_{L3}, are the legs of triangle $t \in \Lambda_t$. N is also the number of triangles in a given mesh.

TABLE I: Performance of LiDAR-camera data mesh generation algorithms

Edge Root Mean Square				
K	0.5	0.7	0.9	0.97
Poisson reconstruction — $O(m^3 log(m))$				
μ	0.00634	**0.00455**	0.00411	0.00419
σ	0.004	**0.003**	0.002	0.002
Alpha Shapes — $O(m^2)$				
μ	0.01522	0.01443	0.01198	0.00929
σ	0.014	0.013	0.012	0.012
Delaunay Triangulation — $O(mlog(m))$				
μ	0.02197	0.02388	0.024193	0.02394
σ	0.052	0.049	0.049	0.051

Table I shows that even when the 3D map data is gathered from a lidar sensor as opposed to RGBD data in [7], Poisson reconstruction is still by far the most optimal mesh generation algorithm. This is proven by the fact that Poisson reconstruction generates triangular mesh with low ERMS indicating the mesh is of high quality and conforms to the environment most optimally. Furthermore, as mentioned in [7], due to the fact that Poisson reconstruction's time complexity is polynomial, an initial subsampling on the pointcloud must be performed

and based on the results in Table I, a subsampling percent (K) equal to 0.7, strikes the best balance.

C. Odometry Results/Comparison

In order to evaluate the effectiveness of the odometry using the data gathered by the LiDAR sensor, a circular route was driven in an indoor environment. From there we are able to visualize the amount of drift that each odometry technique presents without the use of loop closure detection. The results can be visualized in Figure 3. As you will notice the vision based odometry drifted slightly more and lost a lot of the detail/slight movements as compared to LiDAR based odometry. Another important thing to note is that the vision based odometry lost odometry due to lack of landmarks $5\times$ more often than LiDAR based odometry.

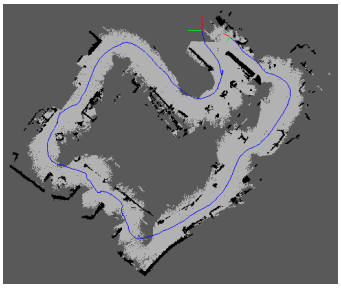

(a) LiDAR-inertial odometry

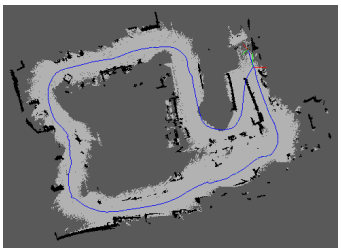

(b) Visual-inertial odometry

Fig. 3: Tracked pose from environmental landmarks using L515 LiDAR Camera

D. Dynamic Simulation on Field Collected Data

Establish the dynamic model of wheelchair in ADAMS / View, with a three-dimensional size of the wheelchair (length $\times$ width $\times$ height) of $1100 \times 700 \times 1300mm$, The wheelbase B of the wheelchair is $600mm$, the wheelbase L of the wheelchair is $560mm$, and the wheelchair's height of the mass centroid from the ground h_s is $440mm$. Taking into account the dynamic model of the wheelchair in the actual use of the user, The mass of the wheelchair model increases the mass of the person so that its total mass is $160kg$ (the mass of the human body is $80kg$). Note that the parameters were selected to best mirror the autonomous wheelchair system described above.

The four tire specifications of the wheelchair are $205/55$ $R16$, this model is a tire model that uses magic formulas and is suitable for wheelchair roll stability analysis. In this case, 3D equivalent volume pavement is selected for simulation pavement, make the real road elevation data collected by the above laser radar into a .rdf road file, Import ADAMS / View to generate 3D road simulation model. as seen in Figure 4.

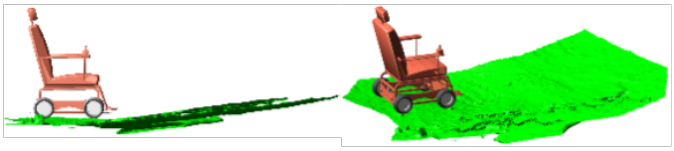

Fig. 4: Wheelchair simulation in ADAMS on field collected data

1) Posture Angle: During the wheelchair driving, the posture angle of the wheelchair's centroid position changes with time as shown in Figure 5. When the wheelchair crosses the stairs, the pitch interval of the wheelchair is about [-20°, 15°], indicating that the wheelchair is always in the climbing process; The change range of the yaw angle is about [-0.35°, 5.5°], indicating that the wheelchair does not produce a relatively large yaw and can still keep driving straight; The change range of roll angle is about [-13°, 8°], which provides intuitive data prediction for anti-rollover control.

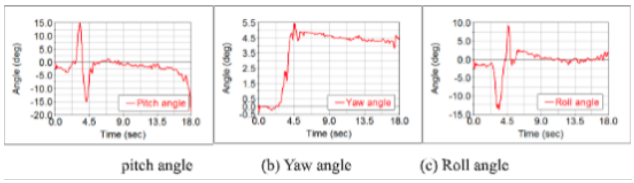

pitch angle (b) Yaw angle (c) Roll angle

Fig. 5: Curve of wheelchair attitude angle with time

2) Curve of Acceleration: Figure 6 is the curve of the acceleration of the centroid position with the time of wheelchair driving. From the figure, we can find: The acceleration of the center of mass of the wheelchair when driving on a flat road is almost 0, which is consistent with the simulation animation. At the last part of the road and when crossing the stairs, the centroid acceleration changes to a certain extent, the maximum vertical acceleration of the wheelchair is about $1g$, and the maximum longitudinal acceleration of the wheelchair is about $1.2g$; The maximum roll acceleration is about $0.75g$, which is used to predict the rollover state of the wheelchair.

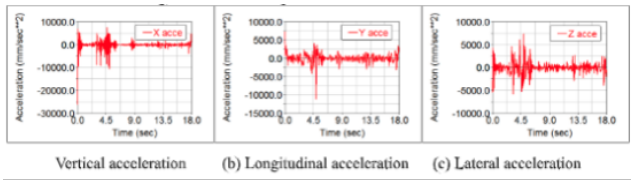

Vertical acceleration (b) Longitudinal acceleration (c) Lateral acceleration

Fig. 6: Curve of centroid acceleration of wheelchair with time

3) Normal Forces on Tires: Figure 7 is the curve of the four tires of the wheelchair during travel with time and it indicates that: when the wheelchair is driving in the rough road and crossing the steps, the four wheels are unevenly stressed and

bumps occur. The stress of the rear wheel is generally higher than that of the front wheel, which is in line with the climbing force of the wheelchair through the steps. In addition, from the normal force of the left and right tires of the wheelchair, the roll state of the wheelchair can be obtained indirectly, which can be used as an indirect prediction criterion for the roll stability of the wheelchair.

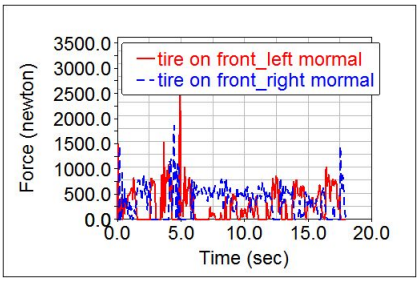

(a) Force on the front wheels

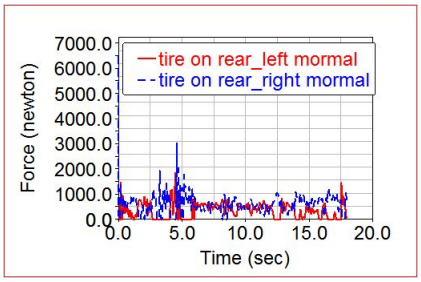

(b) Rear wheel force

Fig. 7: Curve of centroid acceleration of wheelchair with time

VI. Conclusion

In this paper we have deployed a 3D mapping pipeline onto the recently released LiDAR sensor from Intel. By utilizing RTAB mapping and Poisson reconstruction, we are able to construct an accurate representation of the environment that allows for the norms to be extracted for stability analysis. A future area of improvement in our work is the running time for the mesh generation. Although, Poisson reconstruction was selected due to it's distinct characteristic of being resistant to data noise, it presents a poor time complexity that in this paper was dealt with by simply subsampling the 3D pointcloud. Also another interesting area to investigate is the influence of other terramechanical properties of terrain on stability of wheelchairs. The vision of this work is to be integrated into a comprehensive autonomous wheelchair to help enable greater independence/mobility for a population that is handicapped.

References

[1] WHO: Spinal Cord Injury: Fact Sheet (2013)

[2] Khaled, A., Morkos, C., Waheed, D., Hany, S.: Smart obstacle avoidance wheelchair. (2018)

[3] Niijima, S., Sasaki, Y., Mizoguchi, H.: Real-time autonomous navigation of an electric wheelchair in large-scale urban area with 3d map. Advanced Robotics **33**(19) (2019) 1006–1018

[4] Tsykunov, E., Ilin, V., Perminov, S., Fedoseev, A., Zainulina, E.: Coupling of localization and depth data for mapping using intel realsense t265 and d435i cameras. arXiv preprint arXiv:2004.00269 (2020)

[5] Wasenmüller, O., Meyer, M., Stricker, D.: Corbs: Comprehensive rgb-d benchmark for slam using kinect v2. In: 2016 IEEE Winter Conference on Applications of Computer Vision (WACV), IEEE (2016) 1–7

[6] : Lidar camera l515 – intel® realsense™ depth and tracking cameras. https://www.intelrealsense.com/lidar-camera-l515/ (Accessed on 08/20/2020).

[7] Naveen, A., Luo, H., Chen, Z., Li, B.: Predicting Wheelchair Stability While Crossing a Curb Using RGB-Depth Vision. In: International Conference on Computers Helping People (ICCHP) with Special Needs, Springer (2020)

[8] Labbé, M., Michaud, F.: Rtab-map as an open-source lidar and visual simultaneous localization and mapping library for large-scale and long-term online operation. Journal of Field Robotics **36**(2) (2018) 416–446

[9] Murarka, A., Modayil, J., Kuipers, B.: Building local safety maps for a wheelchair robot using vision and lasers. The 3rd Canadian Conference on Computer and Robot Vision (CRV06)

[10] Younes, G., Asmar, D., Shammas, E., Zelek, J.: Keyframe-based monocular slam: design, survey, and future directions. Robotics and Autonomous Systems **98** (2017) 67–88

[11] Zhao, C., Hu, H., Gu, D.: Building a grid-point cloud-semantic map based on graph for the navigation of intelligent wheelchair. 2015 21st International Conference on Automation and Computing (ICAC) (2015)

[12] Nister, D., Naroditsky, O., Bergen, J.: Visual odometry. In: Proceedings of the 2004 IEEE Computer Society Conference on Computer Vision and Pattern Recognition, 2004. CVPR 2004. Volume 1. (2004) I–I

[13] Arun, K., Huang, T., Blostein, S.: Least square fitting of two 3-d point sets. ieee transactions on pattern analysis and machine intelligence, 9 (5): 698-700 (1987)

[14] Cignoni, P., Callieri, M., Corsini, M., Dellepiane, M., Ganovelli, F., Ranzuglia, G.: Meshlab: an open-source mesh processing tool. In: Eurographics Italian chapter conference. Volume 2008., Salerno (2008) 129–136

[15] Loze, M.K., Saunders, R.: Two simple algorithms for constructing a two-dimensional constrained delaunay triangulation. Applied Numerical Mathematics **11**(5) (1993) 403–418

[16] Cholewo, T.J., Love, S.: Gamut boundary determination using alpha-shapes. In: Color and Imaging Conference. Volume 1999., Society for Imaging Science and Technology (1999) 200–204

[17] Tarko, A., Hall, T., Romero, M., Jiménez, C.G.L.: Evaluating the rollover propensity of trucks—a roundabout example. Accident Analysis Prevention **91** (2016) 127–134

[18] Schofield, B., Hagglund, T., Rantzer, A.: Vehicle dynamics control and controller allocation for rollover prevention. 2006 IEEE International Conference on Control Applications (2006)

[19] Levesley, M., Kember, S., Barton, D., Brooks, P., Querin, O.: Dynamic simulation of vehicle suspension systems for durability analysis. Materials Science Forum - MATER SCI FORUM **440-441** (01 2003) 103–110

[20] Candiotti, J., Sundaram, S.A., Daveler, B., Gebrosky, B., Grindle, G., Wang, H., Cooper, R.A.: Kinematics and stability analysis of a novel power wheelchair when traversing architectural barriers. Topics in Spinal Cord Injury Rehabilitation **23**(2) (2017) 110–119

[21] Yu, H., Güvenç, L., Özgüner, : Heavy duty vehicle rollover detection and active roll control. Vehicle System Dynamics **46**(6) (2008) 451–470

[22] Coleman, S., Baker, C.: An experimental study of the aerodynamic behaviour of high sided lorries in cross winds. Journal of Wind Engineering and Industrial Aerodynamics **53**(3) (1994) 401–429

[23] He, Y., Yan, X., Lu, X.Y., Chu, D., Wu, C.: Rollover risk assessment and automated control for heavy duty vehicles based on vehicle-to-infrastructure information. IET Intelligent Transport Systems **13**(6) (Jan 2019) 1001–1010

[24] Sivic, Zisserman: Video google: a text retrieval approach to object matching in videos. Proceedings Ninth IEEE International Conference on Computer Vision (2003)

[25] Bolitho, M., Kazhdan, M., Burns, R., Hoppe, H.: Parallel poisson surface reconstruction. Advances in Visual Computing Lecture Notes in Computer Science (2009) 678–689